Atmospheric Research, 21 (1988) 337–361
Elsevier Science Publishers B.V., Amsterdam — Printed in The Netherlands

Multifractal Simulations and Analysis of Clouds by Multiplicative Processes

D. SCHERTZER and S. LOVEJOY

EERM/CRMD, Météorologie Nationale, 2 Ave. Rapp, Paris 75007 (France)
Physics Dept., McGill University, 3600 University st., Montreal, Que. H3A 2T8 (Canada)

(Received July 14, 1987; accepted after revision October 26, 1987)

ABSTRACT

Schertzer, D. and Lovejoy, S., 1988. Multifractal simulations and analysis of clouds by multiplicative processes. Atmos. Res., 21: 337–361.

Clouds exhibit fractal structures over wide ranges of scale. However, clouds are not geometrical objects: they are produced by highly intermittent fields (e.g. liquid water content). On the other hand, they are rarely isotropic: "texture", stratification, as well as variable (scale-dependent) orientation of structures are common. To deal with such fractal features, we must generalise scale invariance notions beyond the (usual) geometrical self-similar (or even self-affine) notions. We outline the necessary formalism (generalised scale invariance) and show how it can be used to deal with the strongly intermittent fields which result from multiplicative (cascade-type) processes concentrating matter or energy into smaller and smaller scales leading to the appearance of multiple singularities, multiple dimensions and divergences of statistics for these fields.

We illustrate these ideas with radar rain data showing first how to directly estimate the elliptical dimension characterising the stratification, and second, how to determine universal scale-independent (co-)dimension functions that characterise the distribution of the intense rain regions.

RESUME

Les nuages forment des structures fractales sur une très large gamme d'échelles. Ils ne sont pas pour autant des objets purement géométriques: ils sont produits par des champs très intermittents (telle que la densité d'eau liquide). D'autre part, ils sont rarement isotropes: les phénomènes de "texture", de stratification et d'orientations différentielles sont des traits communs. Pour saisir de tels aspects fractals, nous sommes conduits à généraliser les notions d'invariance d'échelles bien au delà du cadre habituel des notions auto-similaires et même auto-affines. Nous résumons le formalisme nécessaire (Invariance d'Echelle Généralisée) et montrons comment il peut être utilisé pour traiter des champs fortement intermittents produits par des processus multiplicatifs

0169-8095/88/$03.50

(tels que les cascades) qui concentrent les flux de matière et d'énergie dans les échelles de plus en plus petites, créant des singularités multiples, des dimensions multiples, et des divergences statistiques.

Nous illustrons ces idées à l'aide de données radar: nous montrons d'une part comment estimer directement la dimension elliptique caractérisant la stratification de la pluie et, d'autre part, comment déterminer des fonctions co-dimensions universelles caractérisant la distribution des régions de pluie intense.

1. INTRODUCTION

Scaling notions are associated with power-law spectra, lack of characteristic scales over wide ranges, and the appearance of fractal dimensions and structures. More precisely, a field is said to be scaling (or scale-invariant) over a range if the small- and large-scale structures are related by scale changing transformations involving only the scale ratio. It is obviously very attractive to deal within such a framework with clouds, since details of a cloud look rather the "same" as the whole cloud.

The above characteristics are common in many areas of geophysics, and, if considered under the general rubric of non-linear variability, constitute a central, and indeed unifying aspect of geophysical systems. In recent years, there has been a series of new developments in our understanding of scaling, including several that were specifically stimulated by geophysical applications (for discussions see: Lovejoy and Schertzer, 1987a; Schertzer and Lovejoy, 1987a). These new ideas involve both the possibility of very general anisotropic types of scaling (necessary, for example to deal with rotation, stratification or "texture"), as well as "multiple scaling" associated with highly intermittent processes. Scaling is thus no longer confined to the notion of self-similarity (the small scale is a reduced copy of the large), nor to the geometric properties of sets of points: multiple scaling involves fields in which the weak and intense regions have different scaling behaviour.

For rain and cloud fields, attractive stochastic alternatives to deterministic modelling — the latter relying extensively on ad-hoc "sub-grid scale parameterisations" and having only a very limited range of explicit scales — have been developed (for relevant surveys see: Waymire and Gupta, 1981; Lovejoy and Schertzer, 1986a) exploiting some of their scaling properties in a fairly simple manner (e.g., Lovejoy and Schertzer, 1985; Waymire, 1985). By simulating rain by the scaling sum of a large number of random increments or "pulses" of different sizes, one is able to produce cloud and rain field simulations, that include texture, clustering, bands, as well as intermittency. Unfortunately, the linear structure of such processes is in sharp contrast with the actual non-linear dynamics.

Indeed, as discussed in the following section and in distinction to these additive processes, the phenomenological cascade models studied in turbulence

(e.g., Novikov and Stewart, 1964) are multiplicative: the large structures multiplicatively modulate the various fluxes (e.g. of energy) at smaller scales. Additive and multiplicative scaling processes are known to be fundamentally different (Schertzer and Lovejoy, 1985a). In the former case called "simple scaling", "scaling of the increments" or "scaling in probability distributions" (e.g., Lovejoy and Mandelbrot, 1985), a single scaling exponent suffices to describe the behaviour of the statistical moments at different scales. In contrast, the latter case called "multiple scaling" requires multiple exponents (e.g., the mean and variance etc. scale differently) and is therefore more general. If we define structures in the field by those regions that exceed a fixed threshold, then additive processes have a single fractal dimension (independent of the threshold), while multiplicative processes have multiple fractal dimensions that decrease as the threshold is increased (Schertzer and Lovejoy, 1983a, 1984, 1985a, 1986, 1987a–c; Frisch and Parisi, 1985; Halsey et al., 1986). In simulating rain, a basic choice must therefore be made between additive and monodimensional, or multiplicative and multidimensional (also called "multifractal") processes.

In this paper, we outline a number of relevant theoretical developments and give examples of the applications. Section 2 gives a fairly non-mathematical overview of scaling notions, and Section 3 gives insights in the way to generate multifractal clouds by multiplicative processes. Section 4 outlines the motivations for generalising scale invariance to anisotropic situations. Sections 5 and 6 give a more precise mathematical formulation, including relations to intermittency, singularities and divergence of high order statistical moments. More detailed developments of the formalism can be found in Schertzer and Lovejoy (1987b,c), and other geophysical applications will be found in the references Schertzer and Lovejoy (1987a). Section 7 discusses some applications to radar rain data and includes two new data analysis techniques: functional box-counting and elliptical dimensional sampling.

2. SIMPLE AND MULTIPLE SCALING

The simplest (geometrical) illustration of scaling and scale invariance is to consider the (apparently "metric", in fact "measurable") notion of dimension of a set of points. The intuitive (and essentially correct) definition is that the number of points $n(L)$ of the set of scale L is given by:

$$N(L) \propto L^D \tag{1}$$

where D is the dimension (e.g. for homogeneously distributed points on a line $n(L) \propto L$, on a plane $n(L) \propto L^2$, but for in-situ meteorological measuring stations $n(L) \propto L^{1.75}$; Lovejoy et al., 1986a,b). More generally, the "volume" (actually the D-dimensional Hausdorff measure of the set) has the same simple scaling (power law) behaviour (see Section 4), and the dimension is important

precisely because it is the scale invariant (independent of L) notion which prescribes how dense are the points of the set (more generally how frequent is a phenomenon etc.).

In geophysical fluid dynamics, the existence of scaling regimes can often be argued directly from the dynamical equations themselves: the only scales associated with the Navier-Stokes equations are a largest scale of energy injection, and a small viscous scale where most of the dissipation occurs. In the atmosphere these scales (along the horizontal) are roughly of the order of thousands of kilometres and several mm, respectively, allowing the possibility of a scaling regime spanning over nine orders of magnitude in scale. Furthermore, the notion of scaling regimes in the atmosphere can be traced back to Richardson (1922, 1926) who suggested a model of atmospheric dynamics involving a self-similar cascade of energy from large to small scales. Since then, scaling ideas have been central to studies of turbulence, a fact that is most notably expressed by the ubiquity of the scaling $k^{-5/3}$ Kolmogorov spectrum of velocity fluctuations in geophysical flows.

The turbulent velocity field (v) affords a convenient example with which to develop the basic scaling ideas. The first scaling of interest might best be called "simple scaling" since it occurs when only one parameter is sufficient to specify the scaling of all the statistical properties. In this case, it can be expressed as (assuming statistical isotropy and translation invariance):

$$\Delta v(l/\lambda) =^{\mathrm{d}} \lambda^{-H} \Delta v(l) \tag{2}$$

where $\Delta v(l) = |v(x+l) - v(x)|$, λ is a scale ratio, $l(=|l|)$ a separation distance, H the (single) scaling parameter. The equality $=^{\mathrm{d}}$ is understood in the sense of probability distributions, hence the scaling of the various high order statistical moments follows:

$$<\Delta v(l/\lambda)^h> = \lambda^{-\xi(h)} <\Delta v(l)^h> \tag{3}$$

with $\xi(h) = hH$, and "$<->$" means "ensemble" average. Since the energy spectrum is the Fourier transform of the covariance, we have a spectrum $k^{-\beta}$ with $\beta = 2H+1$. If one assumes a scale invariant flux of energy (i.e., of a nearly constant density ϵ) to small scales (the non-linear terms in the Navier-Stokes equations conserve this flux, while breaking up large eddies into smaller and smaller sub-eddies), then dimensional analysis gives $\Delta v(l) \propto \epsilon^{1/3} l^{1/3}$, hence, $H = 1/3, \beta = 5/3$. Note that such a behaviour for the velocity field already leads to singular velocity shears (since $\partial v/\partial x \approx \Delta v/l \approx l^{-2/3}$ which diverges as $l \to 0$). The problem of such singular behaviour was first discussed by Leray (1934) and Von Neumann (1949). As we shall see below, it is indeed central to our current understanding of scaling fields, but with a whole hierarchy of singularities.

Kolmogorov (1962) and Obhukov (1962) pointed out that scaling generally

involves an infinite number of parameters ($\xi(h)$ is not generally linear in h). This is a richer and more interesting behaviour called multiple scaling. The simplest way of expressing this is to consider a scale-invariant quantity such as the energy flux density, whose ensemble spatial average is fixed (independent of scale), but is nonetheless (in a given realisation of the cascade process) highly intermittent. This extreme variability or intermittency can be built up step by step in the cascade process in which large eddies modulate *multiplicatively* the flux to smaller and smaller scales (as discussed in Section 6; see schematic diagrams in Figs. 1 and 2). Denote by ϵ_n the density of the flux obtained after n steps of the cascade process of steps ratio λ (the scale of homogeneity is reduced to $l_n = l_0/\lambda^n$, $\lambda > 1$, in Fig. 2: $\lambda = 4$). As the process is going on, ϵ_n becomes more and more singular (i.e., appearance of sharp peaks corresponding to growing singularities) and respects multiple scaling:

$$<\epsilon_n{}^h> = \lambda^{(h-1)C(h)} <\epsilon_0{}^h> \tag{4}$$

$C(h)$ is a convex function which for each moment h, can be interpreted (Schertzer and Lovejoy, 1987b, c) as the *co-dimension* associated with the hth moment (the co-dimension is simply the difference between the fractal dimension of a set and the space in which it is embedded). Indeed, as soon as we "integrate" the limit ϵ (which is no more a function) of the ϵ_n over a set A (of dimension $D(A)$) in order to obtain the flux $\Pi(A)$ of energy on the set A, we obtain a flux with hth divergent moments as soon as $D(A)$ is smaller than $C(h)$. This singular statistics are due to the fact that in such multiplicative

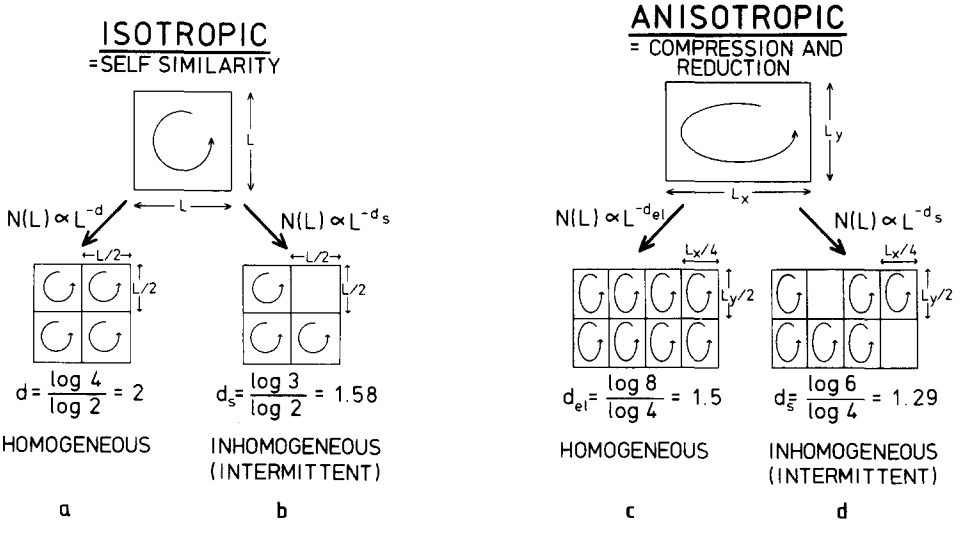

Fig. 1.a. A schematic diagram showing one step of an isotropic homogeneous cascade; b. same as a, but inhomogeneous case; c. same as a for anisotropic case (see Section 3); d. same as c but for inhomogeneous case.

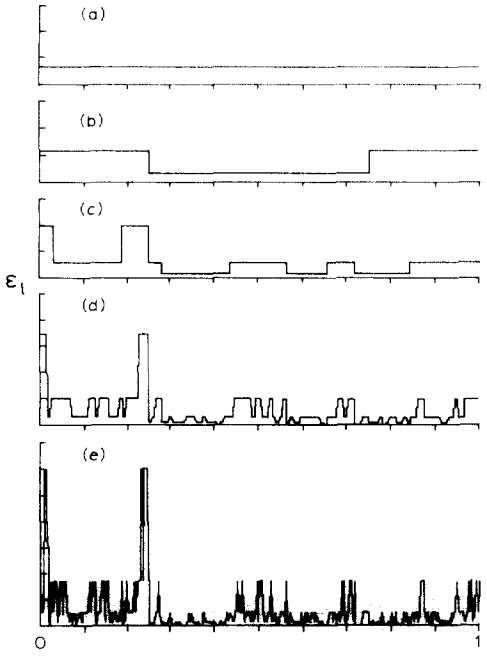

Fig. 2. We show a function which begins by being strictly homogeneous (constant) over the entire interval shown in a, whose scale of homogeneity is then systematically reduced by a successive factor of 4 in b,c,d,e. This is an example of a cascade "α-model" (see Schertzer and Lovejoy, 1985b), which is constructed by multiplying randomly chosen (positive) weights (with only two values: one large and one small) over smaller and smaller scales in such a way that on average, the area under the curve (representing the energy flux to smaller scales) is conserved. Because of this constraint, the increasingly high peaks must become more and more sparse. In the limit of the scale of homogeneity going to zero, the function becomes dominated by singularities distributed over sparse fractal sets.

cascades, singularities of all orders (γ) are built up progressively as the cascade proceeds to smaller scales, hence as $l \to 0$, $\epsilon_l \approx l^{-\gamma}$ with singularities of each order distributed themselves over a (fractal) set of co-dimensions $c(\gamma)$ (see Section 6 for more details). Hence, a scaling field is perceived as a hierarchy of embedded fractals (leading to the expression of multifractal; Frisch and Parisi, 1985). Both families of co-dimensions ($C(h)$ and $c(\gamma)$) are related through a simple (Legendre) transformation.

These surprising mathematical properties of multiplicative processes are themselves associated with a number of interesting phenomena (notably the divergence of high-order statistical moments, explaining the existence of statistical "outliers" in the data), and involve fields that are extremely intermittent with statistical properties depending not only on the scale, but also on the dimension (e.g. line, plane or fractal set) over which they are averaged. This leads to interesting applications to the problem of measurement and calibra-

tion of geophysical data (Lovejoy et al., 1986a,b; Montariol and Giraud, 1986; Lovejoy and Schertzer, 1987b; Marquet and Piriou, 1987).

3. SCALE INVARIANCE AS A PHYSICAL INVARIANCE PRINCIPLE FOR CLOUDS AND RAIN MODELLING

We have pointed out the example of scaling for geophysical fluid dynamics where scaling ideas have been developed over a considerable period of time. Clouds or rain fields are theoretically solutions of complex sets of coupled non-linear partial differential equations including the effect of the dynamical interactions of water vapour and liquid, latent heat release, radiation, wind fields, etc. over a range of over roughly nine orders of magnitude in scale (along the horizontal), and are therefore way beyond the scope of direct deterministic numerical modelling. Even when the dynamical equations are unknown, we can still argue that, at least over certain ranges, these fields respect certain (statistical) symmetries, here scale-changing operations. It must be realised that the requisite scale changes $\boldsymbol{T}_\lambda$ can be far more general than simple (isotropic) reductions. In fact, it turns out that practically the only restriction on $\boldsymbol{T}_\lambda$ is that it has group properties, viz.: $\boldsymbol{T}_\lambda = \lambda^{\boldsymbol{G}}$ where $\boldsymbol{G}$ is the generator of the group (more generally the semi-group) of scale-changing operations. In our "generalised scale invariance" (GSI, see Fig. 3 and Section 5 below), $\boldsymbol{G}$ can be either a matrix ("linear GSI", see Fig. 4a, self-similarity means $\boldsymbol{G}$ = identity),

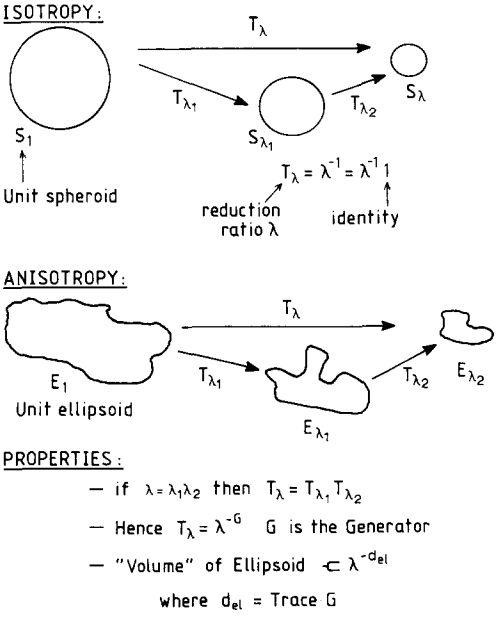

Fig. 3. Schematic illustration of the scaling (semi-)group $\mathbf{T}_\lambda = \lambda^{-\boldsymbol{G}}$.

or a more general non-linear transformation (see Fig. 4b). In fact, it turns out that scale invariance allows for such a tremendous variety of behaviour (i.e., it is only a very weak constraint on the dynamics), that we are just beginning

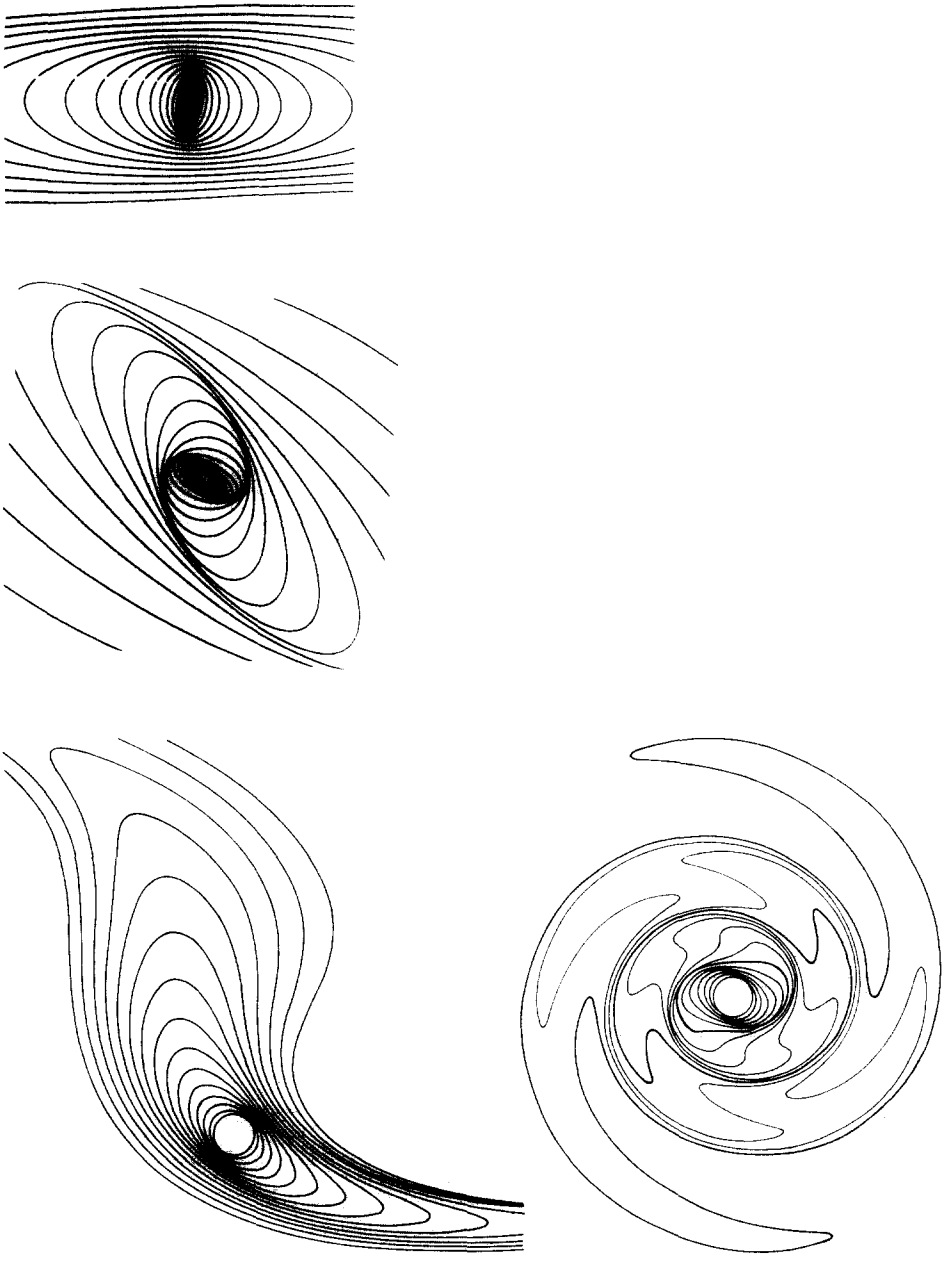

Fig. 4.a. Self-affine balls (with linearly increasing scales). b. Non-linear examples of balls.

exploring. Detailed data analysis and (multi-)fractal models doubtless are required to gain more insight into the relevant dynamics.

As a first step in cloud modelling, it is natural to consider only the dynamical advection processes. The corresponding passive scalar advection has the advantage of being based upon well defined (and studied) equations and phenomenology. It is already sufficiently complex in order to require us to come to grips with some of the basic aspects of the non-linear variability of clouds. Indeed, it is worth noting that in numerical weather prediction models, passive advection of water substance corresponds to the only dynamical process directly taken into account to produce rain; other processes are highly "parameterised". We argue that adding other non-linear effects will not fundamentally change the cascade-type behaviour of the system and the basic modelling techniques will still apply.

In the passive advection of water (concentration ρ) by a velocity field (v), in the limit of vanishing viscosity and diffusivity, the non-linear terms in the dynamical equations conserve the flux of energy and of scalar variance (of respective densities ϵ and χ) while effecting a transfer to smaller scales (hence the cascade). If the injection of these quantities at large scale is constant (or at least a stationary random process), the simplest assumption (going back to Kolmogorov, 1941), is:

$$\left.\begin{aligned} \epsilon &= -<\partial v^2/\partial t> = \text{constant} \\ \chi &= -<\partial \rho^2/\partial t> = \text{constant} \end{aligned}\right| \quad (5)$$

In this framework, ϵ and χ are considered spatial averages over the whole flow (and are denoted by bold script to distinguish them from the local quantities used later) ignoring local variability (which actually turns out to be extreme), and consider that a statistically stationary, relatively homogeneous field of these quantities exists. Then, by dimensional arguments (see Schertzer and Lovejoy, 1987b for a derivation based on the scaling properties of the corresponding equations), we are led to the celebrated scaling laws of Kolmogorov (1941), Obukhov (1949) and Corrsin (1951):

$$\left.\begin{aligned} E_v(\mathrm{K}) &\approx \epsilon^{2/3}\mathrm{K}^{-5/3} \\ E_\rho(\mathrm{K}) &\approx \psi^{2/3}\mathrm{K}^{-5/3} \end{aligned}\right| \quad (6)$$

where $\psi = \chi^{3/2}\epsilon^{-1/2}$ and $E_v(k)$, $E_\rho(k)$ are the power spectra for the velocity and passive scalar fields, respectively, k is a wavenumber ($k \approx 1/l$). ψ is the flux resulting from the non-linear interactions of the velocity and water. Eqs. 6 are satisfied when the velocity and concentration fields are resulting from fractional integrations (i.e., in the Fourier space by multiplying by a non-integer power of the wave-number) over non-intermittent densities of fluxes (e.g., gaussian white-noise). In Schertzer and Lovejoy (1987b), it is proposed to keep on the same line, but with extremely intermittent densities of fluxes pro-

duced by multiplicative processes. Before outlining this proposal, we feel the need to give some insights on scaling anisotropy.

4. ANISOTROPIC SCALE INVARIANCE

A self-similar model of atmospheric fields could not hope to cover more than a very limited range of scales. This is particularly obvious when one considers clouds: extrapolating, by self-similarity, a roughly cubic cloud 1 km in size, to a cloud a thousand kilometres long one would also obtain a cloud a thousand kilometres high! More fundamentally, self-similarity is precluded by the strong atmospheric stratification. The classical schema of atmospheric motions (e.g., Monin, 1972), attempts to overcome this difficulty by considering that atmospheric turbulence is three-dimensional at small scales but (a very different) two-dimensional turbulence at large enough scales. Due to numerous advances in remote and in-situ measurements (see e.g., Lilly, 1983, or Schertzer and Lovejoy, 1985b for reviews) it is now clear that single scaling regimes exist over most of the range of meteorologically significant scales in both the horizontal and vertical directions, although with very different scaling exponents (e.g. horizontal wind has spectral exponents $\beta_h \approx 5/3, \beta_v \approx 11/5$ in the horizontal and vertical directions, respectively).

To avoid this untenable 2D/3D dichotomy, we have proposed an alternative scaling model of atmospheric dynamics (Schertzer and Lovejoy, 1983a,b, 1984, 1985a-c, 1986a,b, 1987a-c; see also Lovejoy and Schertzer, 1986 for a non-mathematical review). In this model, the anisotropy introduced by gravity via the buoyancy force results in a (fractional) differential stratification and a consequent modification of the effective dimension of space, involving a new elliptical dimension (d_{el}), with resulting anisotropic shears. In isotropy, $d_{el}=3$, while in completely flat (stratified) flows, $d_{el}=2$. Empirical and theoretical evidence were given indicating d_{el} is rather the intermediate value:

$$d_{el}=2+(\beta_h-1)/(\beta_v-1)\approx 23/9=2.5555$$

In order to take into account this and other effects such as the differential rotation introduced by the Coriolis force, a general formalism of scaling is required. The fundamental problem is that of finding a family of "balls" representing the statistical properties of the eddies at different scales, via (mathematical) random measures, such as the flux of energy through structures of a given scale. The first step is to generalize the notion of Hausdorff measures and the related (Hausdorff, fractal) dimensions in an anisotropic framework. We recall that such measures are rather straightforward extensions to non-integer D of the Lebesgue measure (defined for integer d), thus we use the notation $\int_A d^D x$ for the D-dimensional Hausdorff measure of a

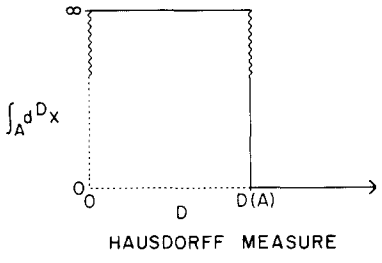

Fig. 5. Divergence rule for Hausdorff measures.

(compact) set A, and we recall that contracting A with a scale ratio λ reduces its measure by the factor λ^D. The Hausdorff dimension $D(A)$ of A is still defined by a divergence rule ("the length of a surface is infinite, the volume of it zero...", see Fig. 5):

$$\int_A d^D x = \infty, \text{ for } D < D(A); \int_A d^D x = 0 \text{ for } D > D(A) \tag{7}$$

It turns out that the divergence of statistical moments derived from a slightly more complex (twin) divergence rule (see Section 6).

5. GENERALISED SCALE INVARIANCE (GSI)

Close examination of the phenomenology of turbulent cascades reveals the basic properties associated with the notion of scale: the (intermittent) concentration of the flux on sparser and sparser regions as the scale of homogeneity goes to zero. Thus scale changing is related to measurable properties of the flow, i.e. how the measure of the energy flux becomes more and more intermittent (less and less homogeneous). We are led to the following abstract definition in terms of a (semi-)group (the "scaling group") of operators $\boldsymbol{T}_\lambda$ which reduce the scale by ratio λ (see Fig. 3 for a schematic illustration):

$$\boldsymbol{T}_\lambda = \lambda^{-\boldsymbol{G}} = \exp(-\boldsymbol{G} \log\lambda) \tag{8}$$

If $\boldsymbol{G}$ is not the identity, $\boldsymbol{T}_\lambda$ is no longer a mere contraction; and the eddies are no longer self-similar (when $\boldsymbol{G}$ is linear, and has no off-diagonal elements, then $\boldsymbol{T}_\lambda$ is self-affine). The consequence of this kind of transformation is that the energy flux is no longer evenly distributed on subsets with equal topological or (isotropic) Hausdorff dimensions. For example, as soon as we anisotropically distribute the activity of turbulence (such as in Fig. 1c, d), a vertical line is no longer equivalent to a horizontal one, etc.

In isotropy, scaling is based on three essential ingredients: (1) a unit sphere; (2) the identity $\mathbf{1}$ as the generator of the self-similar scale changing transfor-

mation, ratio λ ($\boldsymbol{T}_\lambda = \lambda^{-1}$); (3) the resulting scale notion ϕ (which is simply the radius of the sphere S_λ) $\phi(S_\lambda) = \lambda^{-1}\phi(S_1) = \lambda^{-1}$; $S_\lambda = \lambda^{-1}S_1$.

These three ingredients result in the family of self-similar spheres S_λ (the "balls"), whose radii define the scale notion, and are obtained by the scale-changing operation ($\boldsymbol{T}_\lambda$) from one to another ($S_{\lambda'}$ into $S_{\lambda\lambda'}$).

Anisotropic scaling is based on the same ingredients, but with $\boldsymbol{T}_\lambda = \lambda^{-\boldsymbol{G}}$ with $\boldsymbol{G} \neq \boldsymbol{1}$, and $\phi_{\mathrm{el}}(\boldsymbol{T}_\lambda S_1) = \lambda^{-1}\phi_{\mathrm{el}}(S_1)$. The subscript "el" is used in the following to refer to the fact that in anisotropy, the scale-defining spheres are typically flattened ellipsoids (see Fig. 4a). In fact much more general shapes are possible as soon as we use non-linear generators: the balls need not even be convex (Fig. 4b). Using such anisotropic scale-changing operators instead of isotropic

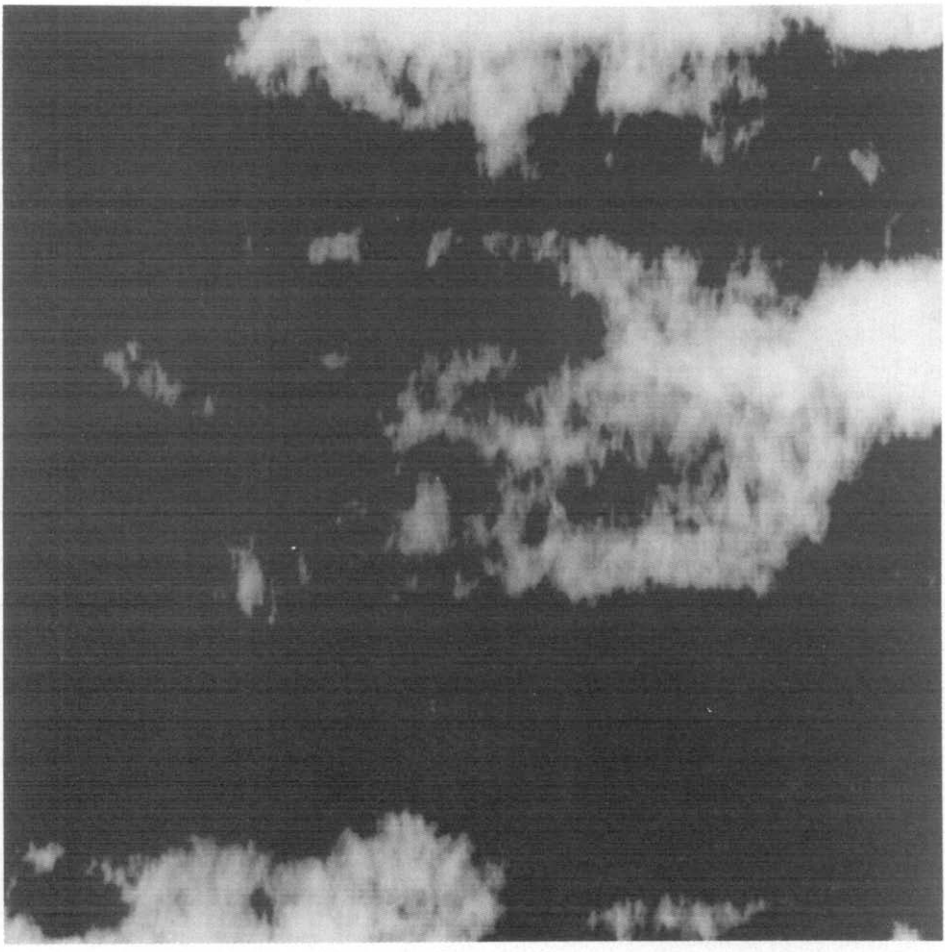

Fig. 6. A cross-section of an anisotropic, fractal-sums-of-pulses process with $d_{\mathrm{el}} = 2.555$.

ones, it is straightforward to transform self-similar stochastic processes into their anisotropic counterparts. Figure 6 gives an example of vertical cloud cross-section obtained by modifying the fractal sums of pulses processes (Lovejoy and Mandelbrot, 1985) so as to simulate a cross-section of a 2.555... dimensional cloud (see Lovejoy and Schertzer, 1985). More elaborate processes (such as those discussed in the following sections) can be rendered anisotropic by using similar techniques. The remaining of the present section (which can be skipped over in a first lecture) gives few indications on the (rather simple) technical ways to solve such a problem.

Indeed, we are thus led to study the properties that a given generator $\boldsymbol{G}$ should satisfy in order that starting from the isotropic triplet $\{S_1, \mathbf{1}, \phi\}$, with $\phi = (\int_A d^d x)\, 1/d$, to the anisotropic $\{S_1, \boldsymbol{G}, \phi_{\text{el}}\}$ the resulting balls $E_\lambda = \boldsymbol{T}_\lambda(S_1)$ correspond to a defined notion of scale (via ϕ_{el}). We are particularly interested in the fact that the E_λ should be decreasing with λ and in a simple definition of ϕ_{el}. It turns out that such conditions (Schertzer and Lovejoy, 1985a, 1987b,c) are satisfied as soon as every (generalised) eigenvalue of $\boldsymbol{G}$ has a non-negative real part, i.e.:

$$\begin{aligned} &\inf \operatorname{Re} \sigma(\boldsymbol{G}) \geq 0 \\ &\sigma(\boldsymbol{G}) = \{\mu \epsilon C | \boldsymbol{G} - \mu \mathbf{1} \text{ non invertible in } CX|R^d\} \end{aligned} \tag{9}$$

$\sigma(\boldsymbol{G})$ being the (generalised) spectrum of $\boldsymbol{G}$ (we recall that in the above definition the usual eigenvalues are included, with the coefficients of the Jordan blocks decomposition) and ϕ_{el} is simply defined as:

$$\phi_{\text{el}}{}^{d_{\text{el}}}(E_\lambda) = \phi^d(E_\lambda) = \lambda^{-d_{\text{el}}} \phi^d(S_1) = \lambda^{-d_{\text{el}}} \phi_{\text{el}}{}^{d_{\text{el}}}(S_1) \tag{10}$$

with $d_{\text{el}} = \operatorname{Tr}(\boldsymbol{G})$ (the trace of $\boldsymbol{G}$) being the "effective" dimension of the space (the anisotropic counterpart of d). Anisotropic Hausdorff measures of dimension D_{el} are simply defined (generalising straightforwardly the definition of the usual isotropic Hausdorff measures) as:

$$\int_A d^{D_{\text{el}}} x = \lim_{\delta \to 0} \inf_{\substack{UE_i \supset A \\ \phi_{\text{el}}(E_i) < \delta}} \sum_i \phi_{\text{el}}{}^{D_{\text{el}}}(E_i) \tag{11}$$

One may note that since (eq. 10) $\phi_{el}{}^{D_{\text{el}}}(\boldsymbol{T}_x S_1) = \phi^D(T_\lambda S_1)$, with $D = (d/d_{\text{el}}) D_{\text{el}}$, $\int_A d^{D_{\text{el}}} x$ is similar (due to eq. 11) to $\int_A d^D x$, notwithstanding the difference that the former case involves a covering by ellipsoids (E_i) rather than spheres (S_i) as in the latter. Nevertheless, if A is not "strange" (pathological), a near optimum covering (i.e. nearly equal to the infimum above) of ellipsoids can be

associated with a near optimum covering of spheres (each of the ellipsoids is itself covered nearly optimally by smaller spheres). We can therefore expect the divergence rule for $\int_A d^{D_{el}}x$ and $\int_A d^{D}x$ to be the same. We have thus the following rule:

$$D_{el}(A)/d_{el} = D(A)/d \tag{12}$$

Nevertheless, it is important to point out exceptions of particular importance: if A is restricted to a (generalised) eigenspace $\boldsymbol{E}_i$ of G, then the preceding rule must be rewritten:

$$D_{el}(A)/d_{eli} = D(A)/d_i \tag{13}$$

where d_i is the topological dimension of $\boldsymbol{E}_i$, d_{eli} its anisotropic dimension defined as the trace of the restriction ($\boldsymbol{G}_{|E_i}$) of $\boldsymbol{G}$ on E_i (i.e., $d_{eli} = \mathrm{Tr}(\mathbf{G}_{|\boldsymbol{E}_i})$).

6. GSI, MULTIPLE SCALING AND SINGULARITIES

Instead of adding random increments of finer and finer resolution along the cascade (as in Fig. 6), one may multiply by random increments of finer and finer resolution. This multiplicative procedure corresponds to a cascade process where the non-linear break-up of eddies into sub-eddies rules the *fraction* of the flux of energy transferred from the eddie scale to the sub-eddies one.

Unlike additive processes where the limit as the inner scale (i.e., the larger scale of homogeneity and at the same time the smaller scale of inhomogeneity) approaches zero is a function, the corresponding limit of multiplicative processes (also called "multiplicative chaos", Kahane, 1985) is very singular. This limit is no longer a function, but an operator converting one measure into another (i.e., the $D(A)$-"volume" of A into the energy flux through A). Indeed, as we introduce finer and finer scale ($l_n = l_0/\lambda^n$) multiplicative perturbations, the density (ϵ_n) of the energy flux becomes increasingly dominated by singularities (positive γ):

$$\epsilon_n \sim {l_n}^{-\gamma};\ \Pr(\epsilon_n \geqslant {l_n}^{-\gamma}) \sim {l_n}^{-c(\gamma)} \tag{14}$$

(see sharp spikes present in Figs. 2, 7) those of higher order than a given level γ, being distributed over a fractal set of co-dimension $c(\gamma)$, becoming sparser with increasing γ (i.e., $c(\gamma)$ is an increasing function). These singularities prevent convergence in the usual sense. However, by "integrating" the result over a set A with dimension $D(A)$ (to obtain the flux through A), the resulting smoothing may be sufficient so that convergence is obtained at least for low-order statistics of the flux. Convergence of statistical moments of order h ($h>1$) is assured by the convergence of the "hth trace moment" (Schertzer and

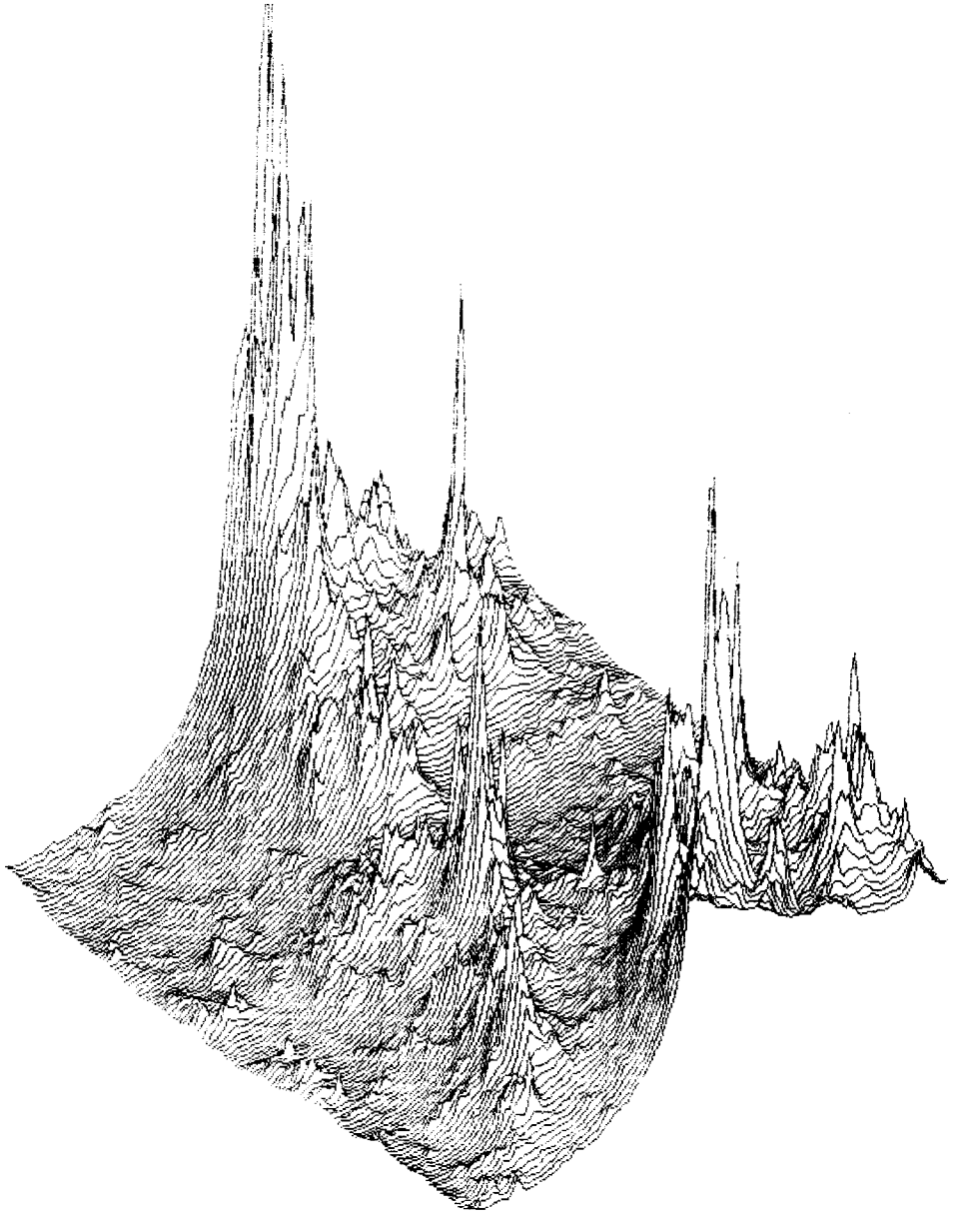

Fig. 7. Multiplicative process on a 128×128 square grid.

Lovejoy, 1987b,c). Here (for simplicity sake), we give only the explicit expressions of approximations to the trace-moments:

$$\langle \mathrm{Tr}_{A_n} \epsilon_n{}^h \rangle = \langle \int_{A_n} \epsilon_n{}^h d^{hD(A)} x \rangle$$
$$\langle \mathrm{Tr}_A \epsilon \rangle \quad = \lim_{n \to \infty} \langle \mathrm{Tr}_{A_n} \epsilon_n{}^h \rangle \tag{15}$$

where A_n is A with a resolution l_n (i.e., we compute the Hausdorff measure, eq. 11, by covering only with balls of size similar to that of the homogeneity scale). Since the latter quantity is of the same type as a Hausdorff measure (Schertzer and Lovejoy, 1987b,c), it is not surprising that it follows a twin divergence rule (represented in Fig. 8), implying the convergence of statistics of order h, for $C(h) < D(A)$ $(h > 1)$ and divergence otherwise, where $C(h)$ is the codimension function defined by the trace moments. Conversely, for $h < 1$, we obtain $C(h) > D(A)$ implying degeneracy of the flux (statistical moments are zero).

Since a multiplicative group (parameter λ, the generalised ratio of scales) is involved, the characterization of its generator γ is fundamental (which different positive values correspond to the different order of singularities). It turns out that it should be "$1/f$ noise" (its spectrum being proportional to the inverse of the wave-number) in order to assure a logarithmic divergence of its "free energy" (or its second characteristic functional) which is required to obtain (multiple) scaling of the resulting field. The co-dimension functions $c(\gamma)$, $C(h)$ are thus related to each other by a Laplace transformation (which reduces to a Legendre transformation, except in divergent cases). Fig. 7 results from a simulation using a gaussian "$1/f$ noise", but Levy noise could also be used. Using this type of continuous cascade construction, it was further shown (Schertzer and Lovejoy, 1987b,c) that continuous cascade processes define universality classes (for fields obtained by fractional integrations over powers of flux densities) in which $c(\gamma)$ is of the form:

$$c(\gamma) = c(0)(\gamma/\gamma_1 + 1)^{\alpha} \tag{16}$$

where, with the value $\alpha = 2$ corresponding to the case of gaussian cascade gen-

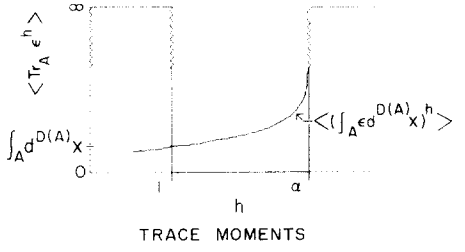

Fig. 8. Twin divergence rule of the trace moments.

erator ($\alpha > 2$, corresponds to a Levy's noise of parameter α': $1/\alpha + 1/\alpha' = 1$), and $c(0)$, γ_1 are parameters characterising, respectively, the intermittency and smoothness of the process.

The codimension functions $c(\gamma)$ and $C(h)$ (determining the fraction of the (sub-)space where singularities or divergences occur) are directly connected to the generator γ of intermittency. Hence, when the latter is expressed in a given framework, defined by the anisotropic generator $\boldsymbol{G}$ with corresponding d_{el} (i.e., γ and $\boldsymbol{G}$ commute), these two functions remain the same for any restriction of the process on a (generalised) eigenspace of $\boldsymbol{G}$ (this is analogous to the isotropic case). This remark is of particular importance for data analysis of anisotropic fields: one may seek to determine the anisotropy generator yielding such an invariance of the codimension functions or at least the corresponding elliptical dimension.

7. ELLIPTICAL DIMENSIONAL SAMPLING AND THE EMPIRICAL EVALUATION OF d_{el} IN RAIN

7.1 The data

In this section we estimate d_{el} and $c(\gamma)$ for radar rain reflectivities. These reflectivities are probably the geophysical data of highest quality available for this purpose. The rain drops act as efficient natural tracers, allowing the 3-D rain structure to be quickly and non-perturbatively sampled. The archives of the McGill weather radar observatory contain data of the radar rain reflectivity (denoted Z) spanning over two orders of magnitude in each horizontal direction, one in the vertical, five in time, and six in intensity. The actual data analysed here were resampled in (r,θ,z) (range, azimuth and height above the earth's surface), from the original polar (r,θ,ϕ) coordinates, with $(200\times375\times8)$ resolution elements, with intensities in 16 logarithmic levels, 4 dBZ apart (factor ~ 2.5). The whole scale therefore spans a range of 15×4 dBZ = 60 dBZ = factor of 10^6, and it is not uncommon for reflectivity levels in rain to exceed 10^5 times the minimum detectable signal.

Physically, the reflectivity is simply the integrated backscatter of the rain drops. The microwave reflectivity for each drop (here at 10 cm wavelength) is proportional to V^2 (where V is the rain drop volume). At 10 cm, the absorption is sufficiently small that the beam is nearly unattenuated. The reflectivity Z measured in this way is the integral over an entire "pulse" volume (roughly 1 km^3) of V^2 of each drop modulated by its phase. Operational (meteorological) use of radar data is limited primarily by the fact that the rain rate (R) is a different integral: that of the product of V and the fall speed. The standard semi-empirical (and very rough) relationship between R and Z is called the Marshall-Palmer formula: $Z = 200\,R^{1.6}$ with Z in (mm)^{6}m^{-3}, and R in mm/h. It is important to note that by directly studying relative reflectivities rather

than R, we avoid the traditional radar calibration problem. Noise and instrumental biases are small.

7.2. *Functional box-counting*

We have to generalise the usual "box-counting" algorithm (designed to estimate the dimension of a set of points, e.g. Hentschel and Proccacia, 1983) so as to apply it to fields ("functional box-counting"). This is achieved (as shown in Fig. 9) by thresholding the fields (with various threshold T_i) and determining the corresponding hierarchy of dimensions $D(T_i)$ (approximating them by $N(L) \sim L^{-D(T_i)}$, $N(L)$ being the number of boxes, of size L, needed to cover the set (defined by those regions exceeding the threshold). From the theoretical discussion of Section 6, and especially eq. 14, this hierarchy of thresholds (T_i) and corresponding dimensions ($D(T_i)$) are related to one of the orders of singularities (γ_i) and its co-dimension function ($c(\gamma_i)$) according to (see Schertzer and Lovejoy, 1987c):

$$T_i \sim L^{-\gamma_i}; c(\gamma_i) = d - D(T_i) \tag{17}$$

When such a functional box-counting is applied to the radar reflectivity data for a single radar scan, we obtain the results shown in Fig. 10. In the horizontal, we have used sectorial (pie-shaped) boxes, increasing the angular and down-range box sizes by factors of 2, starting with the highest resolution available (the use of pie-shaped boxes eliminates all range-dependent effects due to beam

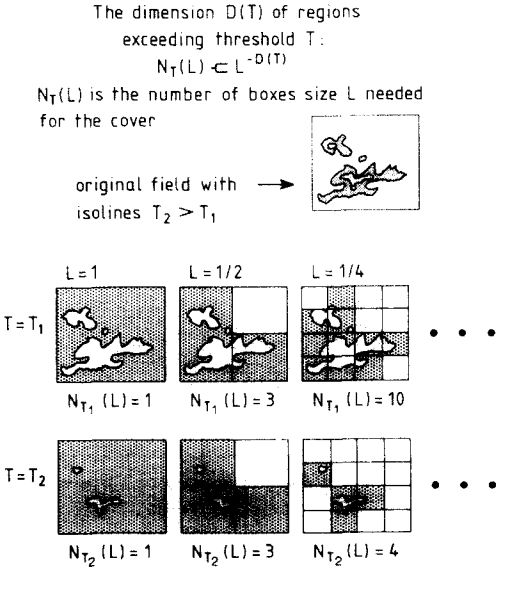

Fig. 9. Functional box-counting.

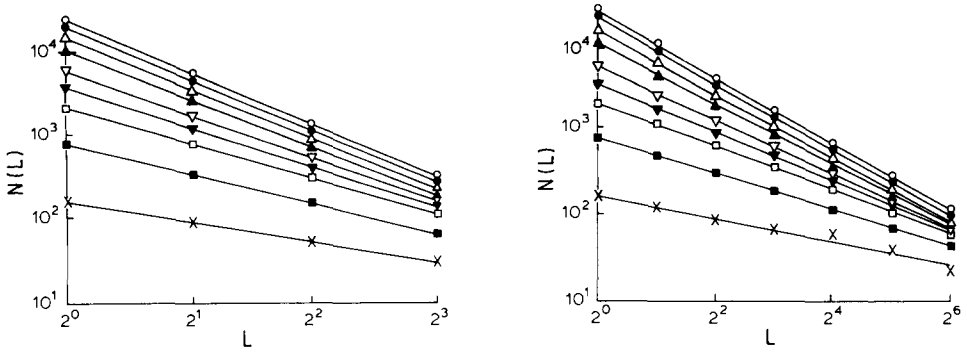

Fig. 10.a. $N(L)$ vs. L for the nine radar reflectivity thresholds discussed in the text, for a single radar volume scan, analysed with horizontal boxes increasing by factors of two in linear scale (data corresponding to a Montreal summer, convective shower). All correlation coefficients of log N vs. log L were >0.99. For clarity, only every second threshold symbol is shown at the left, with values representing the ratio of the reflectivities to the minimum detectable signal. The negative slope, D, decreases from 1.24 to 0.40. b. Same as a, except that the boxes used are cubical (three-dimensional) instead of squares. Here D decreases from 2.18 to 0.81. Only 8 different vertical levels were available.

spreading, etc.). The straightness of the lines shows that scaling is accurately followed in both horizontal and vertical directions. Note the systematic decrease in the absolute slope ($=D(T)$) as T is increased (here through 9 values separated by 4 dBZ — spanning a total range of reflectivity of $10^{(9-1)0.4}$). Of twenty radar volume scans studied, all the horizontal $D(T)$ values calculated by regressions of log $N(L)$ vs. log L resulted in correlation coefficients >0.99, when T was in this range (for the lowest 6 thresholds, where $N(L)$ was fairly large, the correlation coefficient was >0.999). For even higher values of T, $N(L)$ was too small to give reliable estimates of $D(T)$.

Recently, Gabriel et al. (1986, 1987) have applied this technique to visible and infrared satellite pictures of both clouds and surface features in the range 8–512 km. Their results clearly show the scaling of both fields and have important consequences for satellite remote sensing, since scaling generally implies strong (and undesirable) resolution-dependencies in quantities (such as fractional cloud cover) estimated from the satellite. The finding of multiple scaling in visible albedoes and IR emission from (cloud-free) land surfaces confirms that scaling is likely to be a property of many geophysical surface features.

7.3 Elliptical dimensional sampling

We can now apply functional box-counting to horizontal cross-sections and volumes (Fig. 10), determining the functions $D_2(T)$ and $D_3(T)$, respectively, and use the difference between the two to obtain a characterisation of the de-

gree of horizontal stratification in rain. If the rain field was isotropic, then $D_2(T)$, $D_3(T)$ can be simply related to each other by the identity of their corresponding co-dimensions:

$$C_3(T) = C_2(T)$$
$$C_d(T) = d - D_d(T) \tag{18}$$

We have already noted the generalisation of these relations in anisotropy, so that the correct elliptical dimension d_{el} of the rain field should satisfy:

$$C_{del}(T) = C_2(T)$$
$$C_{del}(T) = d_{el} - D_{el}(T) \tag{19a}$$

We thus sample (see Fig. 11) the data using a family of self-affine boxes — with corresponding generators **G**'s and associate elliptical dimensions D_{el}'s — seeking the zero of the following function:

$$f(D_{el}) = \sum_{i=1}^{k} (C_{D_{el}}(T_i) - C_2(T_i)) \tag{19b}$$

with the empirical C's determined by the functional box-counting, and the sum is over the k thresholds ($=9$ here). Furthermore, $f(D_{el})$ is linear in D_{el} due to the linearity of eq. 13.

Fig. 12 shows the result as D_{el} is varied through 15 values between 3 and 2.13, which was roughly the lowest value accessible with the data set, (corresponding to boxes of $1\times1\times1$ pixel and boxes of $190\times190\times2$ pixels; twice the anisotropic scale, where $2.13 = 2 + \log 2/\log 190$). The same nine thresholds were used as before. $f(D_{el})$ was determined separately on 20 radar rain fields: Fig.

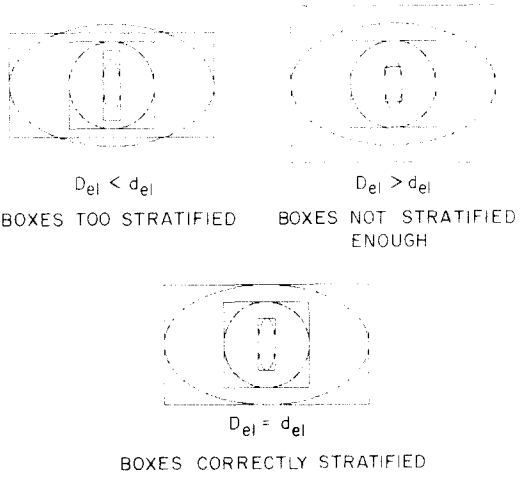

Fig. 11. Elliptical dimensional sampling. Average eddies at three different scales are represented by ellipses, (dimension d_{el}), while the boxes used to analyse the fields are shown as rectangles, (dimension D_{el}). When $D_{el} = d_{el}$ the stratifications of the two are identical.

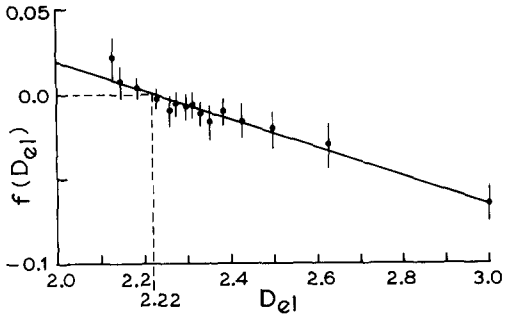

Fig. 12. The function $f(D_{el})$ described in the text which is the average of data taken from 20 scans, using 15 different values of D_{el} and 9 reflectivity thresholds ($=9\times15\times20=2700$ dimensions). The least squares linear regression (correlation coefficient=0.98), is shown, cutting the axis at $D_{el}=d_{el}=2.22$.

12 shows the averages and standard deviations (indicated by the error bars). The linear regression shown, yields $d_{el}=2.22\pm0.07$. The error is the standard deviation of d_{el} estimated from each of the 20 images separately (see Lovejoy et al., 1987 for more details). It is interesting to note that this value is considerably smaller than the value $d_{el}=23/9=2.555...$ found for the horizontal wind field.

7.4 The universality of $c(\gamma)$

In order to estimate the scale invariant (resolution-independent) function $c(\gamma)$ and hence to test the prediction that it has universal form (eq. 16), let us render more precise the eq. 17 by denoting T_L the threshold at scale L (the intrinsic resolution of the detector) associated with the singularity of order γ:

$$T_L/T_0=(L/L_0)^{-\gamma} \tag{20}$$

T_0 is the field value at a reference scale, i.e. the mean field over the entire image.

We now show that the empirical $c(\gamma)$ function fits into the universality classes (eq. 16). For the radar data used here (the same data set discussed in 7.1), the empirically accessible range of γ's is quite small (the maximum is ~2.0). This makes it difficult to accurately estimate α since the latter measures the concavity of $c(\gamma)$ which is only pronounced for large γ. The difficulty is that if eq. 16 is considered to define a multiparameter regression problem for the coefficients $c(0)$, γ_1, α, as determined from the various empirical values $c(\gamma)$, then all three parameters are highly correlated with each other and the optimum values are ill-defined. To obtain well-defined estimates, we therefore made the plausible assumption that generators were in the gaussian domain of attraction (i.e., $\alpha=2$), and for each satellite (and radar) image, we empirically estimated the parameter γ_1 via a least squares regression using the formula:

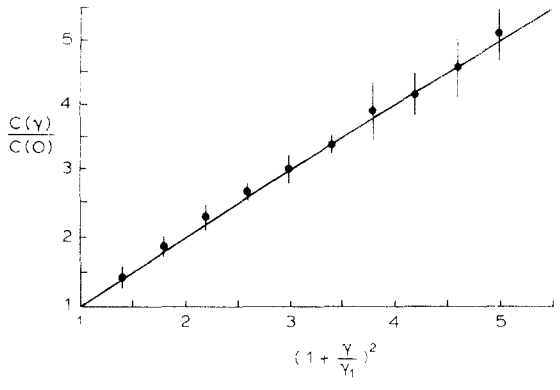

Fig. 13. The mean normalised co-dimension, $<C_N(\gamma)>$ for the radar data, analysed in Fig. 10 (with one standard deviation error bars) plotted against the mean $<(1+\gamma/\gamma_1)^2>$ to test whether the empirical $c(\gamma)$ functions belong to the universality class defined by $\alpha=2$ ($c(0)$ is measured directly, and γ_1 is determined by regression for each image separately). A perfect fit (corresponding to the line $x=y$) is shown for reference.

$$C_N(\gamma)=C(\gamma)/C(0)=(1+\gamma/\gamma_1)^2 \tag{21}$$

where $c_N(\gamma)$ is the co-dimension "normalised" by $c(0)$ which is the empirically determined co-dimension of the field at average brightness (since $T_L=T_0 \Leftrightarrow \gamma=0$). The standard error of the fit (of $c(\gamma)$) in all 20 cases, over the entire range of $c(\gamma)$, was ± 0.062 which is comparable to the errors in determining $c(\gamma)$ from the box-counting algorithm. We then plot the curves $<C_N(\gamma)>$ vs. $<(1+\gamma/\gamma_1)^2>$ in Fig. 13 where the angle brackets indicate ensemble averaging (here all available cases). As predicted by eq. 21, the curves all closely follow the line $x=y$ (shown for reference). This shows that the main difference between the various radar image cases were in the values of the parameters. Similar results (also for $\alpha=2$) for visible and IR satellite images can be found in Gabriel et al. (1987).

8. CONCLUSIONS

We have argued that clouds as anisotropic highly intermittent fields can be best understood and quantitatively studied in the framework of generalised scale invariance (GSI). This formalism is a development of phenomenological models of anisotropic turbulent cascades, but applies generally to anisotropic scale-invariant geophysical fields. Within GSI, singularities of the fields of interest are generated (or analysed in terms of) two multiplicative one-parameter semi-groups. The first defines the anisotropy from scale to scale, and the second, the concentration of the field into sparser and sparser regions, for higher and higher order singularities. The resulting stratification and intermittency have no characteristic scale.

These groups define two (dual) "elliptical" co-dimension functions $C(h)$ and $c(\gamma)$. The former prescribes the divergence of the hth order statistical moments of the flux over regions A of dimension $D(A) < C(h)$ $(h > 1)$ or its degeneracy $(h < 1)$, while the latter describe the distribution of the (multiple) singularities exponents γ.

Multiplicative processes point out features in some respect similar to thermodynamics, but with quite important differences since they correspond to non-equilibrium statistics (the expression "flux dynamics" seems acceptable). For instance, the equivalent of "free energy" (the "free-flux"?) being a $1/f$ noise is unacceptable for thermodynamics, as the divergence of moments. However, some reasonings on the role of symmetries are quite similar. These processes point out the fundamental distinction to be made between theoretical quantities of a partial process (built down to a certain scale of homogeneity of the fluxes) and the "observables" at the same scale (obtained by linear or non-linear integration of a process completed down to an infinitesimal scale of homogeneity): the latter may have statistical divergences (which depend on the dimension of the integration) contrary to the former (which is free from this problem). This distinction must be kept in mind when trying to compare fields computed by a deterministic-type model (with limited range of scales) with real data (averaged on the same scale, largely above the dissipation scale of the process) and may explain most of the usual difficulties encountered: for large fluctuations, small scales play a fundamental role.

To illustrate these ideas, we showed empirical evidence obtained from radar yielding a direct estimate of the elliptical dimension characterising the degree of stratification the rain field: $d_{el} = 2.22 \pm 0.07$. We also determine empirical co-dimension functions that were described by two-parameter universality classes.

9. ACKNOWLEDGEMENTS

We acknowledge discussions with G.L. Austin, P. Gabriel, P. Ladoy, D. Lavallée, E. Levich, J.P. Muller, J.M. Piriou, A. Saucier, A.A. Tsonis, R. Viswanathan, T. Warn. We thank J. Wilson for help preparing Fig. 7. One of us (D.S.) acknowledges support from A.T.P.-C.N.R.S. "Télédétection Spatiale".

10. REFERENCES

Corrsin, S., 1951. On the spectrum of isotropic temperature fluctuation in an isotropic turbulence. J. Appl. Phys., 22: 469–473.

Frisch, U. and Parisi, G., 1985. A multifractal model of intermittency. In: M. Ghil, R. Benzi and G. Parisi (Editors), Turbulence of Predictability in Geophysical Fluid Dynamics and Climate Dynamics. Elsevier, Amsterdam, pp. 84–88.

Gabriel, P., Lovejoy, S., Austin, G.L. and Schertzer, D., 1986. Radiative transfer in extremely variable fractal clouds. 6th Conference on Atmospheric Radiation, AMS, Boston, pp. 230–236.

Gabriel, P., Lovejoy, S. and Schertzer, D., 1987. Fractal characterisation of resolution dependence of satellite radiances. In: D. Schertzer and S. Lovejoy (Editors), Scaling, Fractals and Nonlinear Variability in Geophysics. Reidel, Dordrecht. In press.

Halsey, T.C., Jensen, M.H., Kadanoff, L.P., Procaccia, I. and Shraiman, B.I., 1986. In: Phys. Rev., A, 3(3): 1141.

Hentschel, H.G.E. and Proccacia, I., 1983. The infinite number of generalised dimensions of fractals and strange attractors. Physica, D, 8: 435-444.

Kahane, J.P., 1985. Sur le chaos multiplicatif. Ann. Sci. Math. Que., 9: 435-444.

Kolmogorov, A.N., 1941. Local structure of turbulence in an incompressible liquid for very large Reynolds numbers. Dokl. Acad. Sci. USSR, 30: 299-303.

Kolmogorov, A.N., 1962. A refinement on local structure of turbulence. In: Mécanique de la Turbulence, 447, Editions du CNRS.

Leray, J., 1934. Sur le mouvement d'un liquide visqueux emplisent l'espace. Acta Math., 63: 193-248.

Levitch, E., 1985. Helical fluctuations, fractal dimensions and path integrals in the theory of turbulence. Proc. 199th Euromech. Conf. To appear in: J. Fluid Mech.

Lilly, D.K., 1983. Meso-scale variability of the atmosphere. In: D.K. Lilly and T. Gal'Chen (Editors), Mesoscale Meteorology — Theories, Observations and Models. Reidel, New York, N.Y., pp. 13-24.

Lovejoy, S. and Mandelbrot, B., 1985. Fractal properties of rain and a fractal model. Tellus, 37A: 209-232.

Lovejoy, S. and Schertzer, D., 1985. Generalised scale invariance and fractal models of rain. Wat. Resour. Res., 21: 1233-1250.

Lovejoy, S. and Schertzer, D., 1986. Scale invariance, symmetries, fractals and stochastic simulations of atmospheric phenomena. Bull. AMS, 67: 21-32.

Lovejoy, S. and Schertzer, D., 1987a. Meeting report: Scaling, fractals and non-linear variability in geophysics. EOS, in press.

Lovejoy, S. and Scherzter, D., 1987b. Extreme variability, scaling and fractals in remote sensing: analysis and simulation. In: P.J. Muller (Editor), Digital Image Processing in Remote Sensing. Taylor and Francis, London, in press.

Lovejoy, S., Scherzter, D. and Ladoy, P., 1986a. Fractal characterisation of inhomogeneous geophysical measuring networks. Nature, 319: 43-44.

Lovejoy, S., Scherzter, D. and Ladoy, P., 1986b. Brighter outlook for weather forecasting. Nature, 320: 411.

Lovejoy, S., Schertzer, D. and Tsonis, A.A., 1987. Functional box-counting and multiple elliptical dimensions in rain. Science, 235: 1036-1038.

Mandelbrot, B. 1974. Intermittent turbulence in self-similar cascades: divergence of high moments and dimension of the carrier. J. Fluid Mech., 62: 331-350.

Marquet, O. and Piriou, J.M., 1987. Modélisation fractale des champs de pluie, mesurés par le réseau français. Engineer's Thesis, Météorologie Nationale, Toulouse.

Monin, A.S., 1972. Weather Forecasting as a Problem in Physics. MIT Press, Cambridge, Ma.

Montariol, F. and Giraurd, R., 1986. Engineer's Thesis, Météorologie Nationale, Toulouse.

Novikov, E.A. and Stewart, R., 1964. Intermittency of turbulence and spectrum of fluctuations in energy-dissipation. Izv. Akad. Nauk SSSR, Ser. Geofiz., 3: 408.

Obukhov, A.M., 1949. Structure of thermal fluctuation advected by a turbulent field. Izv. Akad. Nauk SSSR, Ser. Geogr. Geofiz., 13: 58-69.

Obukhov, A. M., 1962. Fluctuations of the energy dissipation in turbulence. J. Geophys. Res., 67: 3011.

Pietronero, L. and Siebesma, A.P., 1986. Self-similarity of fluctuations in random multiplicative processes. Phys. Rev. Lett., 57: 1098-1101.

Richardson, L.F., 1922. Weather Prediction by Numerical Process. Republished by Dover, 1965.

Richardson, L.F., 1926. Atmospheric diffusion shown on a distance neighbor graph. Proc. R. Soc., London, A110: 709–722.

Schertzer, D. and Lovejoy, S., 1983a. The dimension of atmospheric motions. Preprint, IUTAM Symp. Turbulence and Chaotic Phenomena in Fluids. Kyoto, pp. 141–144.

Schertzer, D. and Lovejoy, S., 1983b. On the dimension of atmospheric motions. Proc. 4th Symp. Turbulent Shear Flows, 11.1, 11.8.

Schertzer, D. and Lovejoy, S., 1984. In: T. Tatsumi (Editor), Turbulence and Chaotic Phenomena in Fluids. Elsevier, Amsterdam, pp. 505–508.

Schertzer, D. and Lovejoy, S., 1985a. Generalised scale invariance in turbulent phenomena. P.C.H. J., 6: 623–635.

Schertzer, D. and Lovejoy, S., 1985b. The dimension and intermittency of atmospheric dynamics. In: B. Launder (Editor), Turbulent Shear Flow, 4. Springer, Berlin, pp. 7–33.

Schertzer, D. and Lovejoy, S., 1985c. Generalised scale invariance in rotating and stratified turbulent flows. Proc., 5th Conf. Turbulent Shear Flow, 13.1–13.6.

Schertzer, D. and Lovejoy, S., 1986. Generalised scale invariance and anisotropic intermittent fractals. In: L. Pietronero and E. Tosatti (Editors), Fractals in Physics. Elsevier, Amsterdam, 457 pp.

Schertzer, D. and Lovejoy, S. (Editors), 1987a. Scaling, Fractals and Non-Linear Variability in Geophysics. Reidel, in press.

Schertzer, D. and Lovejoy, S., 1987b. Physical modelling of rain and clouds as anisotropic, scaling and turbulent cascade processes. J. Geophys. Res., 92(D8): 9693–9714.

Schertzer, D. and Lovejoy, S., 1987c. Singularités anisotropes, divergence des moments en turbulence: invariance d'échelle généralisée et processus multiplicatifs. Ann. Sci. Math. (Que.), 11(1): 139–181.

Von Neumann, J., 1949. Recent theories in turbulence. Collected Works, 6: 437–450.

Waymire, E. and Gupta, V.K., 1981. The mathematical structure of rainfall representations, Parts 1–3. Water Resour. Res., 17: 1261–1294.

Waymire, E., 1985. Scaling limits and self-similarity in precipitation fields. Water Resour. Res., 21: 1251–1265.

Yaglom, A.M., 1966. Refinements on log-normal hypothesis of energy dissipation in turbulence. Dokl. Akad. Nauk SSSR, 16: 49.